Atmospheric Environment 161 (2017) 13–17

Contents lists available at ScienceDirect

Atmospheric Environment

journal homepage: www.elsevier.com/locate/atmosenv

Short communication

Ozone production by corona discharges during a convective event in DISCOVER-AQ Houston

Alexander Kotsakis [a], Gary A. Morris [b], Barry Lefer [c], Wonbae Jeon [a], Anirban Roy [a], Ken Minschwaner [d], Anne M. Thompson [e], Yunsoo Choi [a, *]

[a] Department of Earth and Atmospheric Sciences, University of Houston, Houston, TX, USA
[b] St. Edward's University, School of Natural Sciences, Austin, TX, USA
[c] National Aeronautics and Space Administration Headquarters, Washington DC, USA[3]
[d] New Mexico Tech, Department of Physics, Socorro, NM, USA
[e] National Aeronautics and Space Administration, Goddard Space Flight Center, Greenbelt, MD, USA

ARTICLE INFO

Article history:
Received 13 February 2017
Received in revised form
10 April 2017
Accepted 11 April 2017
Available online 13 April 2017

Keywords:
Corona discharge
Lightning
Ozonesonde
Ozone

ABSTRACT

An ozonesonde launched near electrically active convection in Houston, TX on 5 September 2013 during the NASA DISCOVER-AQ project measured a large enhancement of ozone throughout the troposphere. A separate ozonesonde was launched from Smith Point, TX (~58 km southeast of the Houston site) at approximately the same time as the launch from Houston and did not measure that enhancement. Furthermore, ozone profiles for the descent of both sondes agreed well with the ascending Smith Point profile, suggesting a highly localized event in both space and time in which an anomalously large enhancement of 70–100 ppbv appeared in the ascending Houston ozonesonde data. Compared to literature values, such an enhancement appears to be the largest observed to date. Potential sources of the localized ozone enhancement such as entrainment of urban or biomass burning emissions, downward transport from the stratosphere, photochemical production from lightning NO_x, and direct ozone production from corona discharges were investigated using model simulations. We conclude that the most likely explanation for the large ozone enhancement is direct ozone production by corona discharges. Integrating the enhancement seen in the Houston ozone profile and using the number of electrical discharges detected by the NLDN (or HLMA), we estimate a production of 2.48×10^{28} molecules of ozone per flash which falls within the range of previously recorded values (9.89×10^{26} -9.82×10^{28} molecules of ozone per flash). Since there is currently no parameterization for the direct production of ozone from corona discharges we propose the implementation of an equation into a chemical transport model. Ultimately, additional work is needed to further understand the occurrence and impact of corona discharges on tropospheric chemistry on short and long timescales.

1. Introduction

Ozone plays an important role in tropospheric chemistry and driving global climate change. The well-known sources of tropospheric ozone are through photochemistry and stratosphere-troposphere exchange (STE). The sources for photochemical ozone formation are reactions of nitrogen oxides with volatile organic compounds (VOCs) in the presence of ultraviolet radiation. Anthropogenic and biogenic sources constitute the majority of NO_x emissions, with lightning accounting for 10–20% of the global NO_x (Lee et al., 1997). Photochemical production of ozone from lightning NO_x has been well documented in numerous field and remote sensing studies (Lelieveld and Crutzen, 1994; Martin et al., 2007). The amount of ozone produced by lightning NO_x has been estimated to be 1.5 times that transported from the stratosphere (Price et al., 1997).

While ozone is photochemically produced from electrically active storms by lightning NO_x, it can also be produced directly by corona discharges. Compared to high-energy discharges such as cloud-to-ground and cloud-to-cloud lightning, corona discharges occur at lower energies, thus occurring before the conduction breakdowns that lead to lightning strikes. Corona discharges

* Corresponding author.
E-mail address: ychoi23@central.uh.edu (Y. Choi).

http://dx.doi.org/10.1016/j.atmosenv.2017.04.018
1352-2310/

generally will occur on the streamer tips of charge draining regions. Streamers are what connect the areas of opposite charge to each other prior to a lightning discharge. Shlanta and Moore (1972) observed ozone concentrations that were 2.2 and 2.6 times larger than pre-storm surface concentrations just beneath a thundercloud and at an altitude of 6 km respectively. Other observations have shown minimal net production of ozone from corona discharges around thunderstorms due to the significantly larger amounts of NO_x that can also be produced by higher energy discharges (Sisterson and Liaw, 1990). Ozonesonde, aircraft, and ground-based observations around thunderstorms have shown ozone enhancements ranging from 12 to 30 ppbv that was attributed to production by corona discharge (Bozem et al., 2014; Minschwaner et al., 2008; Winterrath et al., 1999).

This study investigates an exceptionally large ozone enhancement observed from an ozonesonde launched near an electrically active convective cell during the National Aeronautics and Space Administration's (NASA) Deriving Information on Surface Conditions from Column and Vertically Resolved Observations Relevant to Air Quality (DISCOVER-AQ) field campaign in Houston on 5 September 2013. To accurately identify the large source of ozone in this study we analyze data from ozonesondes, radar, a lightning mapping array and model simulation output. The findings of this study help in further understanding a source of ozone around convection that has been scarcely observed.

2. Data and methods

2.1. Measurements

Electrochemical concentration type (ECC) (Komhyr, 1986; Komhyr et al., 1995) En-Sci 2Z-V7 ozonesondes (Droplet Measurement Technologies, Boulder, CO) were launched at least once a day from two sites in the Houston, TX area as part of NASA's DISCOVER-AQ field campaign, which took place during September 2013. The primary operating principle of ECC ozonesondes involves an anode and cathode chamber, which contain different concentrations of potassium iodide solution. When ozone enters the cathode chamber, an iodide-iodine redox reaction occurs creating a current, which can be used to derive an ozone concentration. All of the ozonesondes in this study used 0.5% buffered potassium iodide cathode solution as recommended by Smit et al. (2007). With a typical rise rate of ~5 m per second and measurement response time of 20–30 s, the effective vertical resolution of the ozone measurement is 100–150 m. Two launch sites were maintained during DISCOVER-AQ Houston. The first launch site was located at the University of Houston-Main Campus (29.72° N, 95.34° W), an urban site ~3 km south-southeast of downtown Houston and ~8 km west-southwest of the highly industrialized Houston Ship Channel. The second launch site was located at Smith Point, TX (29.55° N, 94.78° W), a rural marine site located on the east side of Galveston Bay. On the afternoon of 5 September 2013, an ozonesonde was launched from Smith Point (SP), TX at 13:20 local time (18:20 UTC) and another ozonesonde was launched from the University of Houston (UH) at 13:47 local time (18:47 UTC). The University of Houston ozonesonde took approximately 57 min to ascend and 45 min to descend and the Smith Point ozonesonde took approximately 113 min to ascend and 27 min to descend. The difference in flight time between the two sites is due to UH launching the ozonesonde with a 350 gram balloon and SP launching with a 600 gram balloon. The larger 600 gram balloon can fly approximately 5 km higher than the 350 gram balloon based on the manufacturer listed burst height specifications, so total flight time with a 350 (600) gram will be shorter (longer). These launch sites are separated by 57.8 km (36 miles), and the launches occurred within 27 min of each other. Each ozonesonde was coupled with an iMet-1-RSB radiosonde (International Met Systems, Grand Rapids, MI), which measured parameters such as temperature, relative humidity, and pressure. A global positioning system (GPS) on the radiosonde provided latitude, longitude, altitude, and wind speed and wind direction derived from the GPS data.

2.2. Lightning and radar data

Data from the Houston Lightning Mapping Array (HLMA) (Cullen et al., 2008) provided horizontal and vertical distribution of lightning discharges. Additional raw lightning data from the U.S. National Lightning Detection Network™ (NLDN) (Cummins et al., 1998) provided data for our ozone calculation. Both the HLMA and NLDN measure cloud-to-ground and cloud-to-cloud lightning discharge by measuring the Very High Frequency (VHF) impulse from the electrical breakdown and lightning propagation processes (Cullen et al., 2008). Base radar reflectivity and enhanced echo top data from the Houston National Weather Service (KHGX) WSR-88D Radar was used for tracking the movement, size, height, and strength of convection.

2.3. Model set up

This study employed the United States Environmental Production Agency (USEPA)'s Community Multi-scale Air Quality (CMAQ) model V5.0.2 (Byun and Schere, 2006). Previous studies have employed the model extensively for simulating and investigating air quality issues around southeastern Texas (Czader et al., 2015; Li et al., 2016). Meteorological inputs were developed using the Weather Research and Forecasting (WRF) model V3.7 (Skamarock and Klemp, 2008). The model domain was set up over the contiguous United States covering 470 × 310 horizontal grid cells. Based on this domain setup, CMAQ and WRF featured a 12 km horizontal grid and a vertical grid extending to 20 km. The USEPA's National Emission Inventory (NEI) for 2011 was used for anthropogenic emissions; these were prepared for modeling using the Sparse Matrix Kernel Emissions Modeling System (SMOKE) V3.6 (Houyoux et al., 2000). Biogenic emissions were estimated using BEIS3 (Biogenic Emission Inventory System version 3) (Pierce et al., 2002). Biomass burning (BB) emissions were taken from the National Center for Atmospheric Research (NCAR)'s (FINN V1.5) Fire Inventory(Wiedinmyer et al., 2011). The inventory was not provided for CMAQ chemical mechanism, and thus the FINN MOZART-4 mechanism was mapped into CB05/AERO6. The model used motor vehicle emissions inputs from the USEPA's Motor Vehicle Emissions Simulator (MOVES) model. The chemical boundary conditions of the domain were taken from the GEOS-Chem output (v10).

3. Results and discussion

The comparison of the observed and modeled vertical ozone profiles for the base (without biomass burning), biomass burning added, and lightning NO_x cases are plotted in Fig. 1. The UH and SP ascent profiles show significant differences in ozone concentrations with the largest differences occurring in the free troposphere (Fig. 1c). The SP ascent profile shows ozone remaining below 100 ppbv throughout the troposphere, while UH ascent profile shows ozone concentrations consistently over 100 ppbv above 4.5 km and over 150 ppbv above 6 km. The Houston profile record (2004-present) does not contain another example with such a large enhancement in the troposphere over such a depth and compared to literature values; such an enhancement appears to be the largest observed to date. While we expected that the boundary layer ozone concentrations between the two sites would be different given

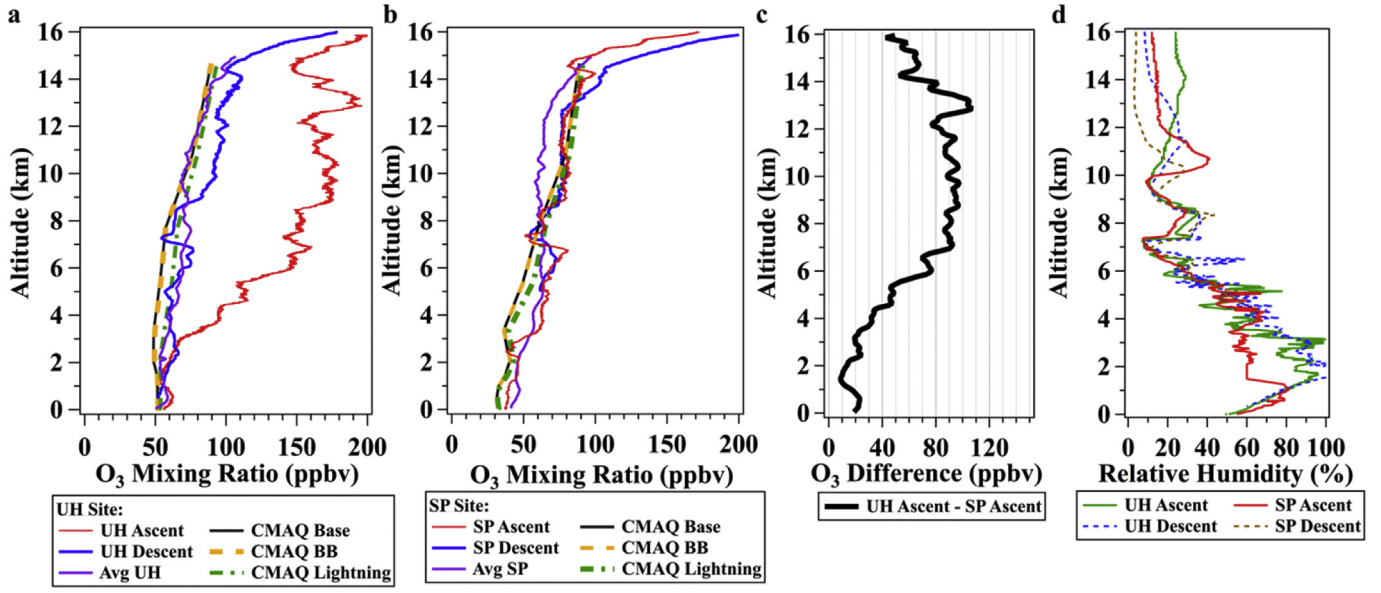

Fig. 1. Ascent (red), descent (blue), and average September profile (purple) data compared to CMAQ model for UH (a) and SP (b) ozonesondes on 5 September 2013. (c) The difference in ozone between the UH and SP ascent profiles. (d) Relative humidity data for the ascent (solid line) and descent (dotted line) of the UH and SP ozonesondes. (For interpretation of the references to colour in this figure legend, the reader is referred to the web version of this article.)

their locations relative to Houston and the Gulf of Mexico (UH being a NO_x-saturated urban site with significant emissions of ozone precursors (NO_x and VOCs), while SP is a NO_x-limited rural site with limited emission sources), we also expected that the concentrations in the synoptically driven free troposphere should be similar due to their proximity to each other. In fact, while a large ozone enhancement is observed by the UH ozonesonde on the ascent, it is not observed on its descent. The UH descent profile is similar to both the SP ascent and descent profiles. This suggests the UH ozonesonde on its ascent measured a highly localized ozone enhancement, while the UH descent, SP ascent, and SP descent profiles were characteristic of the free troposphere in southeast Texas at that time. Additionally, with the exception of the UH ascent profile, the average ozone profiles for September 2013 for each site match well to their respective ascent and descent profiles on 5 September 2013.

A convective cell was formed over Trinity Bay, 55 km east of the UH site, before the launch of either ozonesonde. When the UH ozonesonde was launched, the convective cell was located approximately 48 km (30 miles) to the east over Trinity Bay. Based on radar and ozonesonde GPS data, the storm and the ozonesonde moved east to west at 5–7 m per second and 7–9 m per second respectively. The UH ozonesonde remained ahead of the convection for the entirety of the flight. The SP site and ozonesonde were not impacted by the convection. Data from the NLDN and HLMA showed that this convective cell(s) east of UH were electrically active with substantial lightning discharges.

We investigated several potential sources of this free tropospheric ozone: (1) entrainment of urban or biomass burning emissions, (2) downward mixing from the stratosphere, (3) photochemical production by lightning NO_x, and (4) direct production by corona discharges. Each of these is discussed below.

3.1. Entrainment of urban or biomass burning plumes

When the UH ozonesonde was launched ozone concentrations at the surface ranged between 45 and 55 ppbv across Houston. Based on the magnitude of the enhancement (to concentrations > 100 ppbv) convective transport of surface ozone cannot be responsible. Previous studies have shown the impact of the convective transport of biomass burning emissions on free tropospheric ozone production (e.g. Dickerson et al., 1987). For our study, the CMAQ simulation results for the base and biomass burning cases are not significantly different from one another. Also, fire data records indicate a negligible amount of regional biomass burning in the vicinity of Houston. Hence, the convective transport of urban/biomass emissions did not contribute to the free tropospheric ozone enhancement.

3.2. Stratospheric intrusion

Stratosphere-troposphere exchange (STE) plays a large role in the exchange of chemical species between the troposphere and the stratosphere. Previous work has documented the transport of ozone from the stratosphere around strong convective events (e.g. Barth et al., 2015). Strong to severe convective events primarily observed during the Deep Convective Clouds and Chemistry (DC3) Field Campaign, is in contrast to the sea breeze initiated mesoscale non-severe convective cell in this study. To quantify stratospheric transport, we used the top and upper lateral chemical boundary condition from GEOS-Chem rather than CMAQ due to the latter having a history of under-predicting upper tropospheric ozone (Eder et al., 2010). The GEOS-Chem model has more vertical layers (47 as opposed to 15) for the same height compared to CMAQ making it well suited to capture the stratospheric transport of ozone to the upper troposphere. The lack of a steep positive ozone gradient in the model profiles in Fig. 1, suggests that stratospheric impact is negligible. Relative humidity data from the ozonesonde and potential vorticity (PV) data from the NCEP reanalysis support this conclusion as well. PV is defined as the amount of absolute vorticity between isentropic surfaces within an effective depth. Typically, the troposphere has values less than 2 PV units (PVU), and the stratosphere has values over 2 PVU. High-resolution PV profiles were generated using the NASA Goddard 7 day kinematic back trajectory model (Schoeberl and Sparling, 1993), driven by National Centers for Environmental Prediction (NCEP)

meteorological data for the UH site. The PV profile for September 5th remained below 1 PVU throughout the troposphere, similar to the average profile for August and September 2013 (not shown). Additionally, since stratospheric air is very dry, typically a distinct dry layer is seen in the upper tropospheric relative humidity data if an STE did occur. Fig. 1d shows that the relative humidity on the ascent and descent of the UH ozonesonde does not exhibit any large gradients of very dry stratospheric air in the upper troposphere, proving there is no evidence for large-scale STE influence.

3.3. Photochemical production from lightning NO_x

Lightning NO_x is produced around storms with hot channel intracloud and cloud-to-ground lightning discharges. Photochemical ozone production rates from NO_x, however, are not rapid enough to produce the amount of ozone measured in this case (e.g., Choi et al., 2009). The CMAQ modeling simulation with the default lightning parameterization showed the production of ozone from lightning NO_x could only account for up to ~6 ppbv, far less than the enhancement seen in this case. This missing source of ozone may be accounted for by investigating the direct production of ozone by non-lightning discharges.

3.4. Direct production from corona discharges

We calculate the approximate ozone enhancement due to direct production by corona discharges using Equation 1 from Minschwaner et al. (2008)

$$P(O_3) = DO_3 \times \frac{\Delta Z \cdot A}{N_L} \quad (1)$$

Where DO_3 is the mean ozone enhancement, ΔZ the cylindrical storm volume height, A the cross-sectional storm area, and N_L the number of lightning flashes. The mean ozone enhancement was calculated by using the ascent and descent data from the UH ozonesonde. The cross-sectional area was approximated using the horizontal distribution of detected lightning discharges from HLMA and the spatial coverage of base reflectivity radar data from KHGX. The storm volume height was approximated using the echo tops data from the radar, which provides a value for the altitude of the storm top height. The number of lightning discharges around the convective cell was determined by the NLDN data with only negatively charged discharges being observed. Even in the presence of positive discharges, negative discharges are only considered because negatively charged corona have been found to produce more ozone than positively charged corona (Hill et al., 1988). We calculated an approximate total enhancement of 2.48×10^{28} molecules of ozone per flash. Based on the uncertainties in mean ozone enhancement (±30%) and cylindrical storm volume (+20%, −80%), the approximate range is between 8.73×10^{27} and 3.89×10^{28} molecules of ozone per flash. While this approximation is on the higher end, it is in the range of previous approximates of 9.89×10^{26}–9.82×10^{28} molecules of ozone per flash (Bozem et al., 2014; Minschwaner et al., 2008). However, a different approach described in section 4 is needed to determine the amount of ozone directly produced while also taking into account ozone titration or production from lightning NO_x.

Our hypothesis is that the large amount of ozone observed by the UH ozonesonde was due to direct production of ozone by corona discharges. Corona discharges differ from high-energy return strokes seen with cloud to ground (CG) lightning (Sisterson and Liaw, 1990). Numerous laboratory studies have shown that NO_x is predominately produced in conditions with high temperature (~30,000 K) return strokes (i.e. cloud-to-ground, cloud to cloud) (Franzblau, 1991). Corona discharges, which comparatively are lower in temperature (~300 K) and energy, efficiently produce ozone (Simek and Clupek, 2002). To produce these discharges, the electric field needs to be strong enough to produce a conductive region, but not conductive enough to produce a hot channel discharge. Corona discharges likely occur prior to and during the maturity of the cell when there is a breakdown of the electric field and a subsequent increase in lightning activity. In the presence of predominately hot channel discharges, the environment in and around the storm will be dominated by NO_x production. Due to the proportionally larger amount of hot than cold channel discharges in most storms, the amount of ozone produced compared to NO_x is insignificant. It is possible that the ozone measured on the UH ascent was efficiently produced during the formation of the convection and then transported vertically and horizontally in the convection's growing anvil outflow region. Understanding this interaction between chemistry and lightning discharges associated with convection could be important to understanding the variability in free tropospheric ozone over Houston (Cooper et al., 2006), especially considering Houston has one of the highest annual flash densities in the United States (Orville and Huffines, 2001).

4. Conclusions and future recommendations

This study has presented a unique observation that strongly suggests the influence of corona discharge on ozone production. Two ozonesondes were launched within 58 km and 30 min of each other during the DISCOVER-AQ Houston campaign. Examining the four ozone profiles consisting of the ascending and descending measurements of both sondes, the ascending profile from the UH ozonesonde showed significant enhancements (~100–150 ppbv) relative to the other three. By using observational and modeling approaches, we rule out STE, biomass burning, and transport of the polluted boundary layer into the free troposphere as mechanisms for this case, leaving only direct production from corona discharges.

Currently, there is no parameterization in the chemical transport models to account for this mechanism. An attempt will be made using the approach of Bozem et al. (2014) to try to parameterize direct production of ozone from corona discharges for future use in a chemical transport model.

$$\frac{O_3}{NO}\frac{[excess]}{[excess]} = \frac{O_3\ flash^{-1}}{NO\ flash^{-1}} \quad (2)$$

The proposed parameterization is an improvement from the Minschwaner et al. (2008) equation since it also accounts for lightning NO_x produced around convection. O_3 *[excess]* refers to the amount of excess ozone extracted from experimental data (i.e. ozonesonde or aircraft). NO_x *[excess]* is the amount of excess NO_x that is determined by using experimental data or the difference between CTM runs with the lightning parameterization on and off. The $NO_x\ flash^{-1}$ is a set value that is used in the chemical transport model. $O_3\ flash^{-1}$, which is what will be solved for in the equation, will represent the amount of ozone directly produced by non-lightning discharges. This equation takes into account NO_x production from lightning to determine the amount of ozone produced directly from corona discharges. There are a couple of uncertainties: (1) The amount of NO_x produced per flash has significant uncertainty (2) O_3 [excess] and if possible NO_x [excess] need to be experimentally obtained simultaneously (note that the NO_x [excess] data are not available for this case study). This basic parameterization can be successful if the unknowns are accurately determined and if it can be tested for other case studies. Additional work needs to be done to understand charge distribution and the

complex photochemistry around thunderstorms to properly understand the impact of corona discharges on the tropospheric ozone budget. Future measurements of ozone, NO_x and electrical fields around non-severe convective events are needed to better understand the spatial and temporal impacts of ozone produced by corona discharges. Further modeling work is needed for this case and other potential cases to see if the proposed parameterization works for multiple scenarios.

Acknowledgments

Funding provided by the National Aeronautics and Space Administration through grant NNX10AR39G, Texas Commission on Environmental Quality and the Texas Air Quality Research Program (administered by the University of Texas) through grant UTA12-000894, and the NASA Division of Earth Science 2013 DISCOVER-AQ field project. Thanks to Richard Orville and Gary Huffines for providing lightning data for this case study.

References

Barth, M.C., et al., 2015. The deep convective clouds and chemistry (DC3). Field Campaign. Bull. Amer. Meteor. Soc. 96, 1281–1309. http://dx.doi.org/10.1175/BAMS-D-13-00290.1.

Bozem, H., Fischer, H., Gurk, C., Schiller, C.L., Parchatka, U., Koenigstedt, R., Stickler, A., Martinez, M., Harder, H., Kubistin, D., Williams, J., Eerdekens, G., Lelieveld, J., 2014. Influence of corona discharge on the ozone budget in the tropical free troposphere: a case study of deep convection during GABRIEL. Atmos. Chem. Phys. 14, 8917–8931.

Byun, D., Schere, K.L., 2006. Review of the governing equations, computational algorithms, and other components of the models-3 Community Multiscale Air Quality (CMAQ) modeling system. Appl. Mech. Rev. 59, 51–77.

Choi, Y., Kim, J., Eldering, A., Osterman, G., Yung, Y.L., Gu, Y., Liou, K.N.C.L., 2009. Lightning and anthropogenic NOx sources over the United States and the western North Atlantic ocean. Impact OLR Radiat. Eff. Geophys. Res. Lett. 36, L17806. http://dx.doi.org/10.1029/2009GL039381.

Cooper, O.R., et al., 2006. Large upper tropospheric ozone enhancements above midlatitude North America during summer: in situ evidence from the IONS and MOZAIC ozone measurement network. J. Geophys. Res.-Atmos. 111, 19.

Cullen, M., Rodeheffer, D.R., Krehbiel, P.R., Rison, W., Orville, R.E., 2008. The Houston Lightning Mapping Array: Installation, Operation, and Preliminary Results, 93rd AMS Annual Meeting.

Cummins, K.L., Murphy, M.J., Bardo, E.A., Hiscox, W.L., Pyle, R.B., Pifer, A.E., 1998. A combined TOA/MDF technology upgrade of the US National lightning detection network. J. Geophys. Res.-Atmos. 103, 9035–9044.

Czader, B.H., Choi, Y., Li, X., Alvarez, S., Lefer, B., 2015. Impact of updated traffic emissions on HONO mixing ratios simulated for urban site in Houston, Texas. Atmos. Chem. Phys. 15, 1253–1263.

Dickerson, R.R., et al., 1987. Thunderst. important Mech. Transp. air Pollut. Sci. v 235, 460–464.

Eder, B., Pierce, T., Godowitch, J., Torian, A., Howard, S., 2010. An Evaluation of CMAQ's Performance in the Planetary Boundary Layer and Free Troposphere Using Ozonesondes, 90th American Meteorological Society Annual Meeting, Atlanta, GA.

Franzblau, E., 1991. Electrical discharges involving the formation of NO, NO2, HNO3, and O-3. J. Geophys. Res.-Atmos. 96, 22337–22345.

Hill, R.D., Rahmim, I., Rinker, R.G., 1988. Experimental study of the production of NO, N2O, and O3 in a simulated atmospheric corona. Ind. Eng. Chem. Res. 27, 1864–1869.

Houyoux, M.R., Vukovich, J.M., Coats Jr., C.J., Wheeler, N.M., Kasibhatla, P.S., 2000. Emission inventory development and processing for the Seasonal Model for Regional Air Quality (SMRAQ) project. J. Geophys. Res. 105, 9079–9090.

Komhyr, W.D., 1986. Operations Handbook: Ozone Measurements to 40-km Altitude with Model 4A Electrochemical Concentration Cell (ECC) Ozonesondes (Used with 1680-MHz Radiosondes). NOAA Technical Memorandum ERLARL-149, 1986.

Komhyr, W.D., Barnes, R.A., Brothers, G.B., Lathrop, J.A., Opperman, D.P., 1995. Electrochemical concentration cell ozonesonde performance evaluation during STOIC 1989. J. Geophys. Res.-Atmos. 100, 9231–9244.

Lee, D.S., Kohler, I., Grobler, E., Rohrer, F., Sausen, R., GallardoKlenner, L., Olivier, J.G.J., Dentener, F.J., Bouwman, A.F., 1997. Estimations of global NOx emissions and their uncertainties. Atmos. Environ. 31, 1735–1749.

Lelieveld, J., Crutzen, P.J., 1994. Role of deep cloud convection in the ozone budget of the troposphere. Science 264, 1759–1761.

Li, X.S., Choi, Y., Czader, B., Roy, A., Kim, H., Lefer, B., Pan, S., 2016. The impact of observation nudging on simulated meteorology and ozone concentrations during DISCOVER-AQ 2013 Texas campaign. Atmos. Chem. Phys. 16, 3127–3144.

Martin, R.V., Sauvage, B., Folkins, I., Sioris, C.E., Boone, C., Bernath, P., Ziemke, J., 2007. Space-based constraints on the production of nitric oxide by lightning. J. Geophys. Res.-Atmos. 112, D09309. http://dx.doi.org/10.1029/2006JD007831.

Minschwaner, K., Kalnajs, L.E., Dubey, M.K., Avallone, L.M., Sawaengphokai, P.C., Edens, H.E., Winn, W.P., 2008. Observation of enhanced ozone in an electrically active storm over Socorro, NM: implications for ozone production from corona discharges. J. Geophys. Res.-Atmos. 113, 7.

Orville, R.E., Huffines, G.R., 2001. Cloud-to-ground lightning in the United States: NLDN results in the first decade, 1989-98. Mon. Weather Rev. 129, 1179–1193.

Pierce, T., Geron, C., Pouliot, G., Kinnee, E., Vukovich, J., 2002. Integration of the Biogenic Emissions Inventory System (BEIS3) into the Community Multiscale Air Quality Modeling System. Presented at 25th Conference on Agricultural and Forest Meteorology, 20–24 May, 2002, Norfolk, Virginia. Available at: http://ams.confex.com/ams/pdfpapers/37962.pdf.

Price, C., Penner, J., Prather, M., 1997. NOx from lightning .1. Global distribution based on lightning physics. J. Geophys. Res.-Atmos. 102, 5929–5941.

Schoeberl, M.R., Sparling, L.C., 1993. Trajectory Modelling: Course CXXIV of the International School of Physics Enrico Fermi - Diagnostic Tools in Atmospheric Physics, pp. 289–305.

Shlanta, A., Moore, C.B., 1972. Ozone and point discharge measurements under thunderclouds. J. Geophys. Res. 77 (24), 4500–4510. http://dx.doi.org/10.1029/JC077i024p04500.

Simek, M., Clupek, M., 2002. Efficiency of ozone production by pulsed positive corona discharge in synthetic air. J. Phys. D-Appl. Phys. 35, 1171–1175.

Sisterson, D.L., Liaw, Y.P., 1990. An evaluation of lightning and corona discharge on thunderstorm air and precipitation chemistry. J. Atmos. Chem. 10, 83–96.

Skamarock, W.C., Klemp, J.B., 2008. A time-split nonhydrostatic atmospheric model for weather research and forecasting applications. J. Comput. Phys. 227, 3465–3485.

Smit, H.G.J., et al., 2007. Assessment of the performance of ECC-ozonesondes under quasi-flight conditions in the environmental simulation chamber: insights from the Juelich ozone sonde intercomparison experiment (JOSIE). J. Geophys. Res. 112, D19306. http://dx.doi.org/10.1029/2006JD007308.

Wiedinmyer, C., Akagi, S.K., Yokelson, R.J., Emmons, L.K., Al-Saadi, J.A., Orlando, J.J., Soja, A.J., 2011. The Fire INventory from NCAR (FINN): a high resolution global model to estimate the emissions from open burning. Geosci. Model Dev. 4, 625–641.

Winterrath, T., Kurosu, T.P., Richter, A., Burrows, J.P., 1999. Enhanced O-3 and NO2 in thunderstorm clouds: convection or production? Geophys. Res. Lett. 26, 1291–1294.